

# Thermal order in holographic CFTs and no-hair theorem violation in black branes

Alex Buchel

*Department of Applied Mathematics*

*Department of Physics and Astronomy*

*University of Western Ontario*

*London, Ontario N6A 5B7, Canada*

*Perimeter Institute for Theoretical Physics*

*Waterloo, Ontario N2J 2W9, Canada*

## Abstract

We present a large class of holographic models where the boundary  $\mathbb{R}^{2,1}$  dimensional conformal field theory has a thermal phase with a spontaneously broken global symmetry. The dual black branes in a Poincare patch of asymptotically  $AdS_4$  violate the no-hair theorem.

May 15, 2020

In [1] the authors asked an interesting question whether an “order” (a thermal phase with a spontaneously broken global symmetry) is always lost at high temperatures<sup>1</sup>? There is a number of holographic models known where the answer is “yes”, *i.e.*, there is a critical temperature  $T_{crit}$ , such that for  $T > T_{crit}$  there is a phase with a spontaneously broken global discrete,  $\mathbb{Z}_2$ , symmetry [2–4] or a continuous,  $U(1)$ , symmetry [5]. The holographic models mentioned correspond to boundary quantum field theories with a mass scale: a coupling of a relevant operator in the model [2] or a strong coupling scale of the Klebanov-Strassler gauge theory [6] in [5]. Ultimately, it is this mass scale that determines  $T_{crit}$ .

But is it possible to have an exotic phenomenon of the global symmetry breaking in the ultraviolet (as first suggested in [2]) in a conformal theory? There is no scale to determine  $T_{crit}$ , and the thermal symmetric and the symmetry broken phases must exist for all temperatures. Necessarily, the *distinct* holographic duals to these phases — the black branes with the translationary invariant horizons — would violate the no-hair theorem. The purpose of this note is to present explicit examples of such holographic models. An impatient reader can simply jump to the discussion of the holographic models in **Step3**. Rather, we follow the construction route from massive QFTs.

• **Step1**<sup>2</sup>. Consider the effective four-dimensional gravitational bulk action<sup>3</sup>, dual to a QFT<sub>3</sub> on  $\mathbb{R}^{2,1}$ ,

$$S_{\text{QFT}_3} = S_{\text{CFT}_3} + S_r + S_i = \frac{1}{2\kappa^2} \int dx^4 \sqrt{-\gamma} [\mathcal{L}_{\text{CFT}_3} + \mathcal{L}_r + \mathcal{L}_i], \quad (1)$$

$$\mathcal{L}_{\text{CFT}_3} = R + 6, \quad \mathcal{L}_r = -\frac{1}{2} (\nabla\phi)^2 + \phi^2, \quad \mathcal{L}_i = -\frac{1}{2} (\nabla\chi)^2 - 2\chi^2 - g\phi^2\chi^2, \quad (2)$$

where we split the action into a conformal part  $S_{\text{CFT}_3}$ ; its deformation by a relevant operator  $\mathcal{O}_r$ ; and a sector  $S_i$  involving an irrelevant operator  $\mathcal{O}_i$  along with its mixing with  $\mathcal{O}_r$  under the renormalization group flow, specified by a constant  $g$ . In all our numerical analysis we set  $g = -100$ . The precise value of  $g$  does not matter, as long as  $g$  is sufficiently negative, see [2]. The four dimensional gravitational constant  $\kappa$  is related to a central charge  $c$  of the UV fixed point as

$$c = \frac{192}{\kappa^2}. \quad (3)$$

---

<sup>1</sup>As in [1], we consider equilibrium phases of the theories without a chemical potential for the conserved global  $U(1)$  symmetries.

<sup>2</sup>This is a review of [2].

<sup>3</sup>We set the radius of an asymptotic  $AdS_4$  geometry to unity.

We assume the scaling dimension of  $\mathcal{O}_r$  to be  $\Delta_r = 2$ . The scaling dimension of  $\mathcal{O}_i$  is  $\Delta_i = 4$ . Generically, we turn on the non-normalizable coefficient of  $\phi$ , corresponding, the nonzero coupling  $\Lambda$  of the dual operator  $\mathcal{O}_r$ . The effective action (1) has a  $\mathbb{Z}_2 \times \mathbb{Z}_2$  discrete symmetry that acts as a parity transformation on the scalar fields  $\phi$  and  $\chi$ . The discrete symmetry  $\phi \leftrightarrow -\phi$  is explicitly broken by a relevant deformation of the CFT<sub>3</sub>; while the  $\chi \leftrightarrow -\chi$  symmetry is broken spontaneously.

The thermal states of the QFT<sub>3</sub> are dual to the black brane solutions in (1) with translationary invariant horizons:

$$ds_4^2 = \frac{\alpha^2 a(x)^2}{(2x - x^2)^{2/3}} \left( -(1-x)^2 dt^2 + [dx_1^2 + dx_2^2] \right) + g_{xx} dx^2, \quad \phi = \phi(x), \quad \chi = \chi(x), \quad (4)$$

where the radial coordinate  $x \in (0, 1)$ . The constant  $\alpha$  is an arbitrary scale parameter, and the metric warp factor  $g_{xx}$  is determined algebraically from  $a, \phi, \chi$ . Solving the equations of motion from (1) and (2) with the background ansatz (4), we find,

$$\begin{aligned} a &= 1 - \frac{1}{40} p_1^2 x^{2/3} - \frac{1}{18} p_1 p_2 x + \mathcal{O}(x^{4/3}), \\ \phi &= p_1 x^{1/3} + p_2 x^{2/3} + \frac{3}{20} p_1^3 x + \mathcal{O}(x^{4/3}), \\ \chi &= \chi_4 \left( x^{4/3} + \left( \frac{1}{7} g - \frac{3}{70} \right) p_1^2 x^2 + \mathcal{O}(x^{7/3}) \right), \end{aligned} \quad (5)$$

near the  $AdS_4$  boundary  $x \rightarrow 0_+$ , and

$$a = a_0^h + a_1^h y^2 + \mathcal{O}(y^4), \quad \phi = p_0^h + \mathcal{O}(y^2), \quad \chi = c_0^h + \mathcal{O}(y^2), \quad (6)$$

near the black brane horizon  $y = 1 - x \rightarrow 0_+$ . Apart from the overall scaling factor  $\alpha$ , a black brane solution is specified with the three UV coefficients  $\{p_1, p_2, \chi_4\}$  and the four IR coefficients  $\{a_0^h, a_1^h, p_0^h, c_0^h\}$ . The UV parameter  $p_1$  determines the coupling constant of the relevant operator  $\mathcal{O}_r$  as

$$\Lambda \equiv p_1 \alpha, \quad (7)$$

while the remaining parameters determine the Hawking temperature  $T$  of the black brane, its entropy density  $s$ , the energy density  $\mathcal{E}$ , and the free energy density  $\mathcal{F}$  as follows:

$$\begin{aligned} \left( \frac{8\pi T}{\Lambda} \right)^2 &= \frac{6(a_0^h)^3(6 - 2(c_0^h)^2 + (p_0^h)^2 - g(p_0^h)^2(c_0^h)^2)}{p_1^2(3a_1^h + a_0^h)}, \quad \frac{\hat{s}}{\Lambda^2} \equiv \frac{384}{c} \frac{s}{\Lambda^2} = \frac{4\pi(a_0^h)^2}{p_1^2}, \\ \frac{\hat{\mathcal{E}}}{\Lambda^3} &\equiv \frac{384}{c} \frac{\mathcal{E}}{\Lambda^3} = \frac{1}{p_1^3} \left( 2 - \frac{1}{6} p_1 p_2 \right), \quad \frac{\hat{\mathcal{F}}}{\Lambda^3} \equiv \frac{384}{c} \frac{\mathcal{F}}{\Lambda^3} = \frac{384}{c} \frac{\mathcal{E} - Ts}{\Lambda^3}. \end{aligned} \quad (8)$$

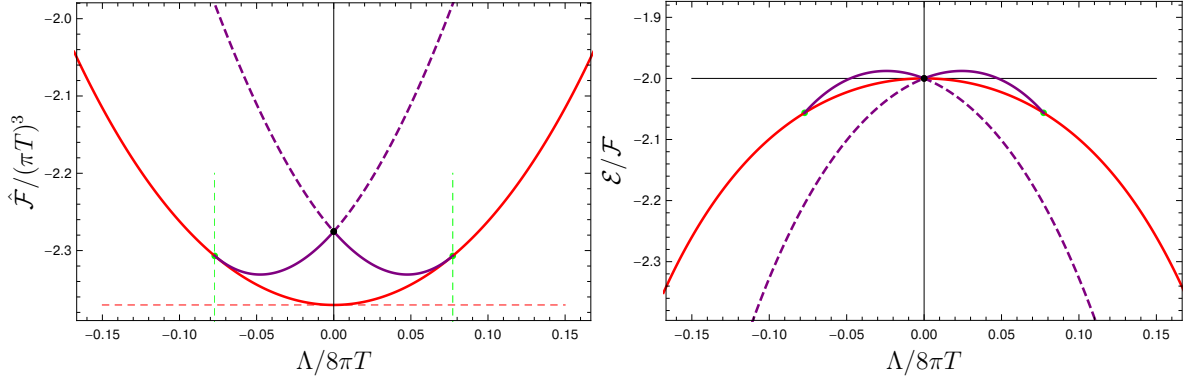


Figure 1: Thermal phases of the QFT<sub>3</sub> with a dual holographic gravitational action (1). The left panel shows the free energy density  $\hat{\mathcal{F}}$ , see (8), and the right panel shows  $\mathcal{E}/\mathcal{F}$  as a function of  $\Lambda/8\pi T$ . At  $\Lambda = 0$  the theory has  $\mathbb{Z}_2 \times \mathbb{Z}_2$  global symmetry. This symmetry is broken to  $\mathbb{Z}_2$  at  $\Lambda \neq 0$  — represented by the red curves. The purple curves represent phases with the spontaneously broken  $\mathbb{Z}_2$  symmetry. They connect with the second order phase transition (green dots, vertical dashed green lines) to a symmetric phase at  $T_{crit} \propto \Lambda$ , see (12). The symmetry broken phases (solid purple curves) exist for  $T \geq T_{crit}$  all the way to the infinite temperature. The infinite temperature phase — represented by a black dot — is our first example of the CFT<sub>3</sub> with spontaneously broken global symmetry, see (13). The symmetry breaking phases can be smoothly extended past the infinite temperature (alternatively across  $\Lambda = 0$ ) — denoted by the purple dashed curves.

Additionally, the thermal expectation values of the operators  $\mathcal{O}_r$  and  $\mathcal{O}_i$  are given by

$$\langle \mathcal{O}_r \rangle \propto \langle \hat{\mathcal{O}}_r \rangle = p_2, \quad \langle \mathcal{O}_i \rangle \propto \langle \hat{\mathcal{O}}_i \rangle = \chi_4. \quad (9)$$

The latter expectation value, *i.e.*,  $\chi_4$ , serves as an order parameter for the spontaneous breaking of the global  $\mathbb{Z}_2$  symmetry.

We briefly review the numerical procedure used to collect the data for the thermal phases of the model (1), reported in figs. 1-3, see [2] for additional details:

- The red curves in figs. 1-3 represent the  $\mathbb{Z}_2$  symmetric thermal phase. Here, the bulk scalar  $\chi(x) \equiv 0$ , correspondingly with  $\chi_4 = 0$  in the UV, see (5), and  $c_0^h = 0$  in the IR, see (6). We use the shooting method first employed in [7] to produce data sets  $\{p_2, a_0^h, a_1^h, p_0^h\}$  from varying  $p_1$ , related to  $\frac{T}{\Lambda}$ , see (8). Specifically, given  $p_1$ , we numerically solve the pair of the coupled second-order ODEs for  $a$  and  $\phi$  from the UV

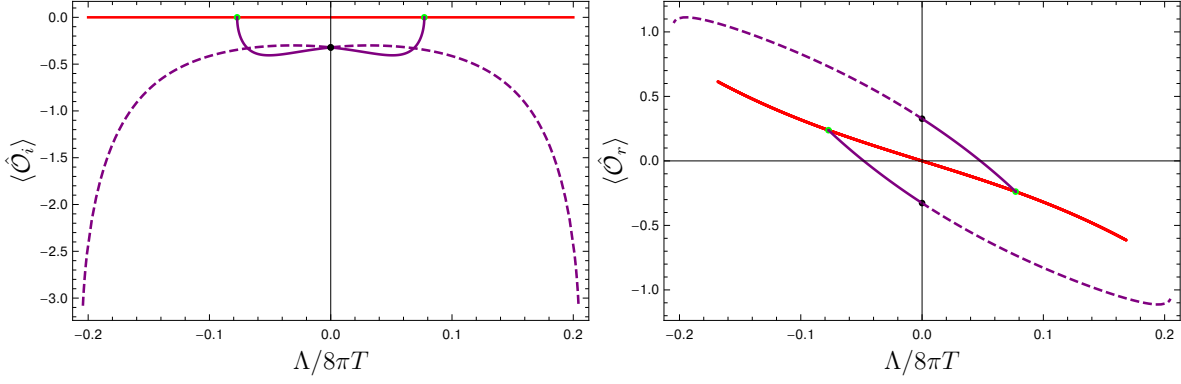


Figure 2: The left panel: the order parameter  $\langle \mathcal{O}_i \rangle$  for the spontaneous breaking of the global  $\mathbb{Z}_2$  symmetry in the QFT<sub>3</sub>. The right panel: the thermal expectation value of  $\langle \mathcal{O}_r \rangle$  in the QFT<sub>3</sub>. The color coding is the same as in fig. 1.

for  $x \in (0, \frac{1}{2}]$  and IR for  $y = (0, \frac{1}{2}]$ , using the corresponding asymptotic expansions (5) and (6), and adjust  $\{p_2, a_0^h, a_1^h, p_0^h\}$  to ensure the continuity of  $a, \phi$  and their first derivatives at  $x = y = \frac{1}{2}$ . From the collected data we compute the thermodynamics of the symmetric phase using (8). The speed of the sound waves in plasma, see fig. 3, is obtained numerically evaluating the derivative

$$c_s^2 = -\frac{\partial \mathcal{F}}{\partial \mathcal{E}} = -\frac{\frac{d}{dp_1} \frac{\hat{\mathcal{F}}}{\Lambda^3}}{\frac{d}{dp_1} \frac{\hat{\mathcal{E}}}{\Lambda^3}}. \quad (10)$$

■ The purple curves in figs. 1-3 represent the thermal phases of the model (1) with the spontaneous breaking of the  $\mathbb{Z}_2$  symmetry, *i.e.*, with  $\chi_4 \neq 0$ . Here, we need to solve three coupled second-order ODEs for  $\{a, \phi, \chi\}$ . Given  $p_1$ , the asymptotic expansions (5) and (6) are characterized by  $\{p_2, \chi_4, a_0^h, a_1^h, p_0^h, c_0^h\}$ . Once again we employ the shooting method of [2]. In practice, to ensure that we obtain solutions with  $\chi_4 \neq 0$ , we fix initially  $\chi_4 = -1$  and obtain from the shooting algorithm the corresponding set  $\{p_1, p_2, a_0^h, a_1^h, p_0^h, c_0^h\}$ . Additional data sets are obtained from this *initial* set varying  $p_1$  (in small increments), as for the symmetric phase. A remarkable fact, that was not appreciated in [2], is that we can vary  $p_1$  in the symmetry broken phase through  $p_1 = 0$  (represented by a black dot in figs. 1 and 2). According to (8), see the expression for  $\frac{T}{\Lambda}$ , this corresponds to reaching an infinitely high temperature and *extending past the infinite temperature* (at fixed  $\Lambda$ ), or alternatively crossing  $\Lambda = 0$ , *i.e.*, the conformal point. Turns out that there are two distinct thermal phases with the spontaneously

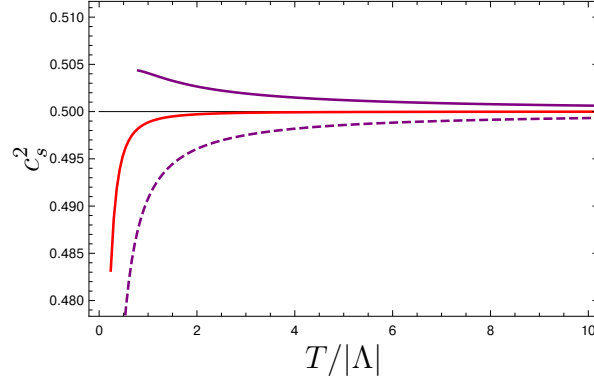


Figure 3: The speed of the sound waves in various equilibrium phases of the QFT<sub>3</sub> plasma. The color coding is the same as in fig. 1.

broken  $\mathbb{Z}_2$  symmetry: we use the solid purple curves to denote the phase with the speed of the sound waves  $c_s^2 > \frac{1}{2}$ , and the dashed purple curves to denote the phase with the speed of the sound waves  $c_s^2 < \frac{1}{2}$ , see fig. 3.

A selection<sup>4</sup> of thermal phases of the QFT<sub>3</sub> is presents in fig. 1. Notice that the horizontal axes correspond to  $\Lambda/(8\pi T)$ , so the region close to the origin corresponds to high temperatures, *i.e.*,  $T \gg \Lambda$ . We show<sup>5</sup> the  $\mathbb{Z}_2$  symmetric phases with  $\langle \hat{\mathcal{O}}_i \rangle = 0$  (red curves) and the symmetry broken phases  $\langle \hat{\mathcal{O}}_i \rangle \neq 0$  (purple curves). The left panel shows the reduced free energy density  $\hat{\mathcal{F}}$ , see (8). Note that for the  $AdS_4$ -Schwarzschild black brane

$$\left. \frac{\hat{\mathcal{F}}}{(\pi T)^3} \right|_{red, \Lambda=0} = -\frac{64}{27}, \quad (11)$$

denoted by a red dashed horizontal line. The solid purple curves connect to the red curve with the second-order transition, green dots, at

$$T_{crit} = 0.515597 |\Lambda| : \quad \lim_{T \rightarrow T_{crit}} \langle \mathcal{O}_i \rangle = 0, \quad (12)$$

denoted by the green dashed vertical lines. As discovered in [2], the symmetry broken phases exist only in the UV, *i.e.*, for  $T \geq T_{crit}$ . They extend to infinitely high temperatures, denoted by the black dot. The black dot is our first example of the CFT<sub>3</sub> with

<sup>4</sup>There is a tower of the symmetry broken thermal phases similar to those discussed here [2].

<sup>5</sup>In all cases we verified that the first law of thermodynamics  $0 = d\mathcal{E}/(Tds) - 1 \Big|_{\Lambda=\text{const}}$  is true numerically to  $\sim 10^{-10}$  or better.

the spontaneously broken global discrete symmetry, in this particular case  $\mathbb{Z}_2 \times \mathbb{Z}_2$ :

$$\text{CFT}_3 : \quad \frac{\hat{\mathcal{F}}}{(\pi T)^3} = -2.275317, \quad \langle \hat{\mathcal{O}}_r \rangle = \pm 0.326946, \quad \langle \hat{\mathcal{O}}_i \rangle = \pm 0.321581, \quad (13)$$

where the uncorrelated  $\pm$  signs represent the 4-fold degeneracy of the symmetry broken phases.

In any thermal phase, symmetric or symmetry broken, the equation of state of a  $\text{CFT}_3$  is  $\mathcal{E} = -2\mathcal{F}$ . In the right panel of fig. 1 we plot  $\mathcal{E}/\mathcal{F}$  in the  $\text{QFT}_3$  as a function of  $\Lambda/8\pi T$ : both the red curve and the purple curves pass through  $(-2)$  in the UV (with a numerical accuracy of  $\sim 10^{-11}$ ).

The symmetry broken phases (solid purple curves) can be smoothly extended “past the infinite temperature” — the dashed purple curves. We have been able to reliably construct the dashed purple phases only for  $|\Lambda|/(8\pi T) \lesssim 0.2043$ .

In fig. 2 we present the order parameter  $\langle \hat{\mathcal{O}}_i \rangle$  for the spontaneous breaking of the global  $\mathbb{Z}_2$  symmetry (the left panel), and the thermal expectation value of  $\langle \hat{\mathcal{O}}_r \rangle$  (the right panel). The color coding is the same as in fig. 1. Notice that as one lowers the temperature along the dashed purple curves, the absolute value of the order parameter sharply increases as  $|\Lambda|/(8\pi T) \rightarrow 0.2043$ . This is the main reason why we could not extend these phases to low temperatures<sup>6</sup>.

In fig. 3 we present the speed of the sound waves in various thermal phases of the  $\text{QFT}_3$  plasma. The color coding is the same as in fig. 1. All the equilibrium phases, symmetric and with the spontaneously broken  $\mathbb{Z}_2$  symmetry, are thermodynamically and dynamically stable [8]. The speed of the sound waves approach a conformal value in the limit  $T/\Lambda \rightarrow \infty$ .

An example of a  $\text{CFT}_3$  with a spontaneously broken  $\mathbb{Z}_2 \times \mathbb{Z}_2$  — the black dot phase in fig. 1 — has a larger free energy density than that of the symmetric phase, dual to the  $AdS_4$  -Schwarzschild black brane:

$$\left. \frac{\hat{\mathcal{F}}}{(\pi T)^3} \right|_{black\ dot} > \left. \frac{\hat{\mathcal{F}}}{(\pi T)^3} \right|_{red, \Lambda=0}. \quad (14)$$

Thus, this phase is metastable<sup>7</sup>. In what follows, we ask the question whether we can introduce an additional “knob” in a holographic model (1) to potentially reverse

---

<sup>6</sup>We expect that the corresponding black branes have a singular horizon in this limit.

<sup>7</sup>It would be extremely interesting to understand the dynamics of the first order phase transition, in particular, to compute the wall tension of the symmetric phase bubble in the symmetry broken thermal phase.

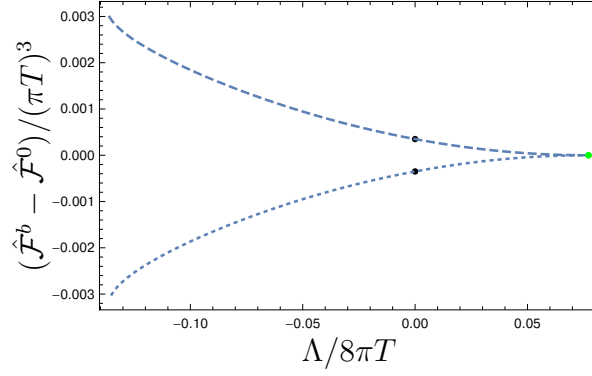


Figure 4: The reduced free energy densities  $\hat{\mathcal{F}}^b$  of the  $\mathbb{Z}_2$  symmetry broken thermal phases of the  $\text{QFT}_3^b$  model, see (15), compare to the free energy density  $\hat{\mathcal{F}}^0$  of the corresponding phases of the  $\text{QFT}_3$  model, see (1). The dashed curve corresponds to  $b = 1$  and the dotted curve corresponds to  $b = -1$  deformation parameter. The green dot indicates the  $b$ -independent critical temperature  $T_{crit}$ , see (12). The black dots represent new examples of  $\text{CFT}_3^b$  with spontaneously broken  $\mathbb{Z}_2 \times \mathbb{Z}_2$  global symmetry.

the inequality (14), and have a symmetry broken phase to dominate in a canonical ensemble<sup>8</sup>. This leads up to **Step2**.

- **Step2.** Consider a smooth constant  $b$  parameter deformation of the model (1):

$$S_{\text{QFT}_3} \rightarrow S_{\text{QFT}_3^b} \quad \Longleftrightarrow \quad \mathcal{L}_i \rightarrow \mathcal{L}_i^b \equiv -\frac{1}{2}(\nabla\chi)^2 - 2\chi^2 - g\phi^2\chi^2 - b\chi^4, \quad (15)$$

with the remaining parts of the effective action left unchanged. Note that the  $\text{QFT}_3^b$  has the same global symmetries as the  $\text{QFT}_3$ . Additionally, the second-order phase transitions associated with the spontaneous breaking of  $\mathbb{Z}_2$  symmetry ( $\chi \leftrightarrow -\chi$ ) happens at  $T_{crit}$  given by (12), independent of the deformation parameter  $b$ .

It is straightforward to repeat the analysis of the thermal phase diagram of the model. In the thermodynamic relations (8) there is only one change<sup>9</sup>:

$$\left(\frac{8\pi T}{\Lambda}\right)^2 = \frac{6(a_0^h)^3(6 - 2(c_0^h)^2 + (p_0^h)^2 - g(p_0^h)^2(c_0^h)^2 - b(c_0^h)^4)}{p_1^2(3a_1^h + a_0^h)}. \quad (16)$$

In fig. 4 we show the effect of the deformation parameter  $b$  on the reduced free energy density  $\hat{\mathcal{F}}^b$  of the symmetry broken phase in the  $\text{QFT}_3^b$  model, compare to the

<sup>8</sup>No examples of such models known.

<sup>9</sup>Of course, all the UV and IR parameters  $\{p_2, \chi_4, a_0^h, a_1^h, p_0^h, c_0^h\}$  will develop an implicit  $b$  dependence.



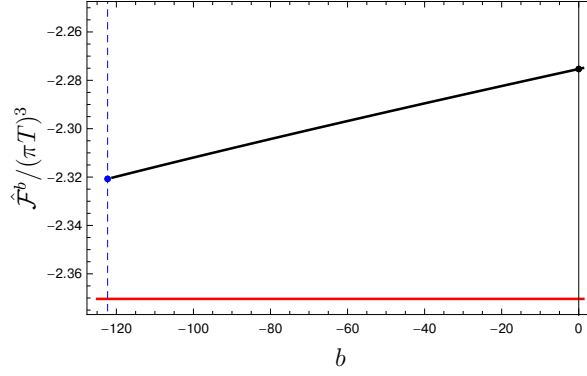


Figure 5: The reduced free energy density  $\hat{\mathcal{F}}^b$  in the  $\text{CFT}_3^b$  model as a function of the deformation parameter  $b$  (the solid black line). The black dot represents the same symmetry broken conformal phase as the black dot in fig. 1. The  $\text{CFT}_3^b$  symmetry broken phase exists only for  $b \geq b_{crit}$ , see (17), denoted by a vertical dashed blue line — it terminates with a blue dot  $\text{CFT}_3^\chi$ , see (19). The horizontal red line represents the reduced free energy density of the  $AdS_4$ -Schwarzschild black brane.

corresponding free energy density in the  $\text{QFT}_3$  model, denoted by  $\hat{\mathcal{F}}^0$  (this is the solid magenta curve in the left panel of fig. 1). The dashed curve corresponds to  $b = 1$  and the dotted curve corresponds to  $b = -1$ . They originate from the same green dot, representing the critical temperature  $T_{crit}$ , as in (12). Following the symmetry broken phases in the  $\text{QFT}_3^b$  model to infinitely high temperature, we identify conformal phases,  $\text{CFT}_3^b$ , with the spontaneously broken  $\mathbb{Z}_2 \times \mathbb{Z}_2$  global symmetry — these are the two black dots in fig. 4. Since we want to reduced the free energy density as much as possible, we now study  $\text{CFT}_3^b$  models for  $b < 0$ <sup>10</sup>.

In fig. 5 we follow (the solid black curve) the free energy density in the  $\text{CFT}_3^b$  model from  $b = 0$  (represented by the black dot — the same black dot as in fig. 1) for  $b < 0$ . The horizontal red line is the value of the free energy density for the  $AdS_4$ -Schwarzschild black brane, see (11). We find that the  $\text{CFT}_3^b$  model allows for a symmetry broken phase only for

$$b \geq b_{crit} = -122.272. \quad (17)$$

The critical value of the deformation parameter is denoted by a vertical dashed blue

---

<sup>10</sup>Notice that the gravitational scalar potential in (15) is unbounded for  $b < 0$ . This does not immediately signal any pathologies — many scalar potentials in top-down supersymmetric holographic models are unbounded. See [4] for further discussion.

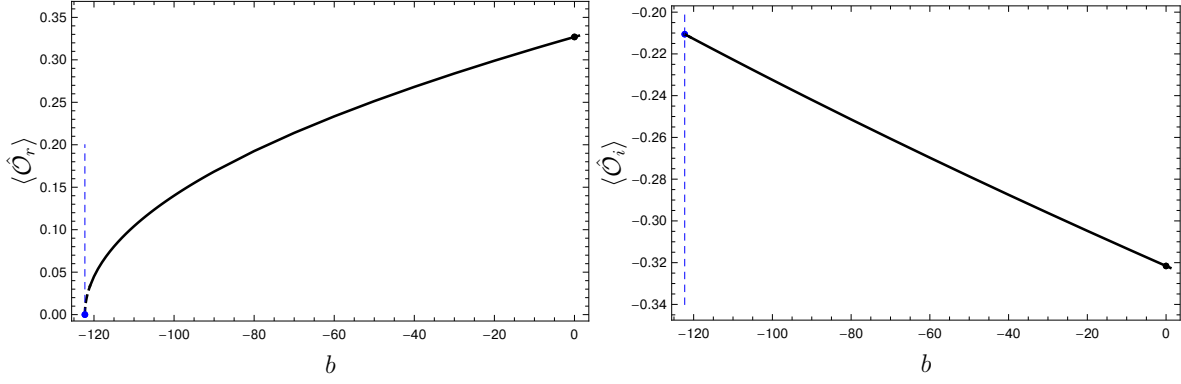


Figure 6: The symmetry breaking order parameters  $\langle \hat{\mathcal{O}}_r \rangle$  and  $\langle \hat{\mathcal{O}}_i \rangle$  in the  $\text{CFT}_3^b$  model as a function of  $b$ . The  $\langle \hat{\mathcal{O}}_r \rangle$  order parameter vanishes as  $b \rightarrow b_{crit}$ , denoted by the vertical dashed blue lines. However, the  $\langle \hat{\mathcal{O}}_i \rangle$  order parameter remains finite at  $b = b_{crit}$  (the blue dot).

line.

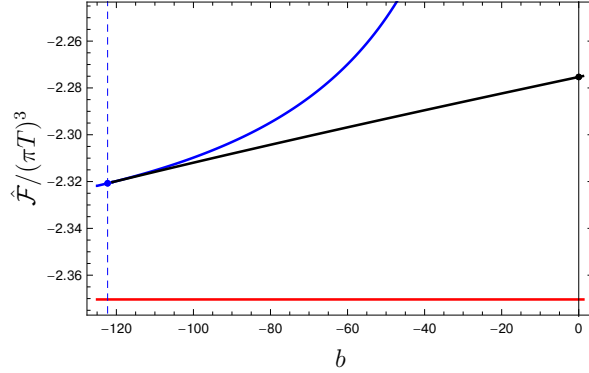


Figure 7: Same as in fig. 5, with the addition of the symmetry breaking phase in the  $\text{CFT}_3^x$  model, see (21) — the solid blue curve.

The origin of  $b_{crit}$  is easy to understand as we follow the symmetry breaking order parameters  $\langle \hat{\mathcal{O}}_r \rangle$  and  $\langle \hat{\mathcal{O}}_i \rangle$  in the  $\text{CFT}_3^b$  model, see fig. 6. We find that while  $\langle \hat{\mathcal{O}}_i \rangle$  remains finite in the limit  $b \rightarrow b_{crit}$ ,

$$\langle \hat{\mathcal{O}}_r \rangle \propto (b - b_{crit})^{1/2}. \quad (18)$$

Thus, precisely at  $b = b_{crit}$  the black brane dual to the  $\text{CFT}_3^b$  symmetry broken phase "loses" the  $\phi$ -hair, while maintaining the non-vanishing  $\chi$ -hair. We call this "terminal"

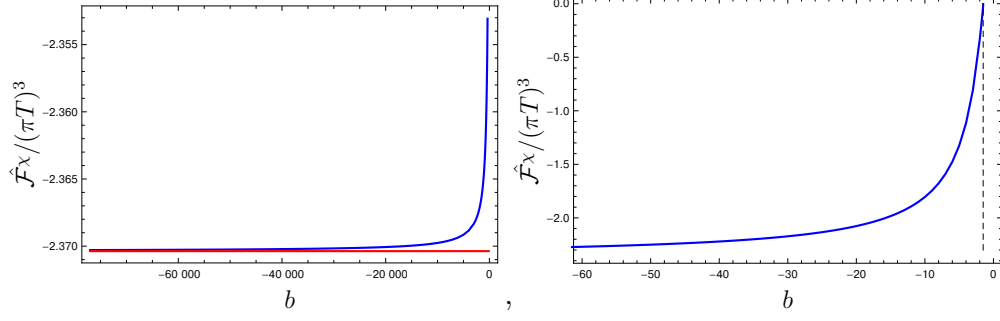


Figure 8: The reduced free energy density  $\hat{\mathcal{F}}^\chi$  of the  $\mathbb{Z}_2$  symmetry broken phase as a function of  $b$ . This phase exists only for  $b < -\frac{3}{2}$ , represented by a vertical dashed black line in the right panel. The horizontal red line represents the reduced free energy density of the  $AdS_4$ -Schwarzschild black brane.

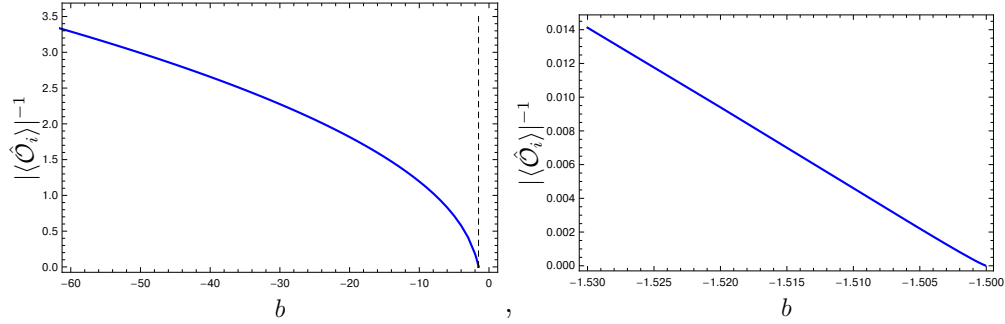


Figure 9: The inverse of the order parameter  $|\langle \hat{\mathcal{O}}_i \rangle|$  for the symmetry breaking in the  $CFT_3^\chi$  model as  $b \rightarrow -\frac{3}{2}_-$ .

conformal model  $CFT_3^\chi$ ,

$$\begin{aligned}
 CFT_3^\chi \Big|_{b=b_{crit}} &\equiv \lim_{b \rightarrow b_{crit}} CFT_3^b, \\
 CFT_3^\chi \Big|_{b=b_{crit}} : \quad \frac{\hat{\mathcal{F}}^\chi}{(\pi T)^3} \Big|_{b=b_{crit}} &= -2.32074, \quad \langle \hat{\mathcal{O}}_i \rangle \Big|_{b=b_{crit}} = \pm 0.21057,
 \end{aligned} \tag{19}$$

where again the  $\pm$  signs indicate the 2-fold degeneracy due to the spontaneously broken  $\mathbb{Z}_2$  global symmetry.

Once again,

$$\frac{\hat{\mathcal{F}}^\chi}{(\pi T)^3} \Big|_{b=b_{crit}} > \frac{\hat{\mathcal{F}}}{(\pi T)^3} \Big|_{AdS_4-Schwarzschild}. \tag{20}$$

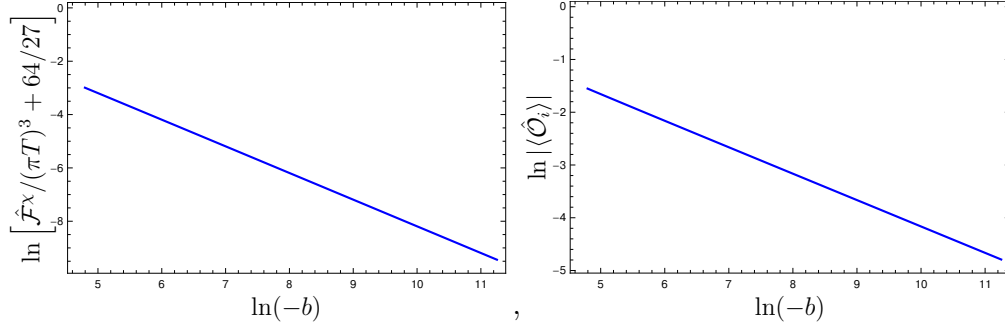


Figure 10: The reduced free energy density of the symmetry broken phase in the  $\text{CFT}_3^\chi$  model always exceeds that of the symmetric phase. It approaches the latter as  $\propto \exp b$  in the limit  $(-b) \rightarrow \infty$ , see the left panel. In the right panel we show the  $\propto (-b)^{-1/2}$  scaling of the symmetry breaking order parameter in the  $\text{CFT}_3^\chi$  model in the limit  $(-b) \rightarrow \infty$ .

Can we do better with relaxing  $b = b_{crit}$  constraint directly in the  $\text{CFT}_3^\chi$  model? This leads us to **Step3**.

- **Step3.** Consider a gravitational dual to  $\text{CFT}_3^\chi$  model,

$$S_{\text{CFT}_3^\chi} = \frac{1}{2\kappa^2} \int d^4x \sqrt{-\gamma} \left[ R + 6 - \frac{1}{2} (\nabla \chi)^2 - 2\chi^2 - b\chi^4 \right], \quad (21)$$

Clearly, the  $S_{\text{CFT}_3^\chi}$  model is a consistent truncation of the  $S_{\text{QFT}_3^b}$  model with  $\phi \equiv 0$ . The  $\text{CFT}_3^\chi$  model has only  $\mathbb{Z}_2$  global symmetry. The symmetry broken blue dot phase in fig. 5 must also be a solution of the effective action (21), except that now we are not restricted to keep  $b = b_{crit}$ . In fig. 7 the solid blue curve traces the free energy density of the symmetry broken phase in the  $\text{CFT}_3^\chi$  model as a function of the parameter  $b$  in (21).

The thermal phase with the spontaneously broken  $\mathbb{Z}_2$  symmetry exists in the  $\text{CFT}_3^\chi$  model for  $b \leq -\frac{3}{2}$ , see fig. 8.

As  $b \rightarrow -\frac{3}{2}_-$ , the order parameter for the symmetry breaking diverges as, see fig. 9,

$$|\langle \hat{\mathcal{O}}_i \rangle| \propto \frac{1}{-3/2 - b}, \quad \text{as} \quad b \rightarrow -\frac{3}{2}_-. \quad (22)$$

Notice that

$$\frac{\hat{\mathcal{F}}^\chi}{(\pi T)^3} > \frac{\hat{\mathcal{F}}}{(\pi T)^3} \Big|_{\text{AdS}_4\text{-Schwarzschild}}, \quad (23)$$

for all value of  $b$ , see fig 10. We find that as  $b \rightarrow -\infty$ ,

$$\frac{\hat{\mathcal{F}}^\chi}{(\pi T)^3} = \frac{\hat{\mathcal{F}}}{(\pi T)^3} \Big|_{AdS_4-Schwarzschild} + \exp \mathcal{C} \left( \frac{1}{\sqrt{-b}} \right)^2, \quad |\langle \hat{\mathcal{O}}_i \rangle| \propto \frac{1}{\sqrt{-b}}, \quad (24)$$

where  $\mathcal{C} \approx 1.81$ .

## Acknowledgments

Research at Perimeter Institute is supported by the Government of Canada through Industry Canada and by the Province of Ontario through the Ministry of Research & Innovation. This work was further supported by NSERC through the Discovery Grants program.

## References

- [1] N. Chai, S. Chaudhuri, C. Choi, Z. Komargodski, E. Rabinovici and M. Smolkin, *Thermal Order in Conformal Theories*, 2005.03676.
- [2] A. Buchel and C. Pagnutti, *Exotic Hairy Black Holes*, *Nucl. Phys. B* **824** (2010) 85–94, [0904.1716].
- [3] P. Bosch, A. Buchel and L. Lehner, *Unstable horizons and singularity development in holography*, *JHEP* **07** (2017) 135, [1704.05454].
- [4] A. Buchel, *Singularity development and supersymmetry in holography*, *JHEP* **08** (2017) 134, [1705.08560].
- [5] A. Buchel, *Klebanov-Strassler black hole*, *JHEP* **01** (2019) 207, [1809.08484].
- [6] I. R. Klebanov and M. J. Strassler, *Supergravity and a confining gauge theory: Duality cascades and chi SB resolution of naked singularities*, *JHEP* **08** (2000) 052, [hep-th/0007191].
- [7] O. Aharony, A. Buchel and P. Kerner, *The Black hole in the throat: Thermodynamics of strongly coupled cascading gauge theories*, *Phys. Rev. D* **76** (2007) 086005, [0706.1768].
- [8] A. Buchel, *A Holographic perspective on Gubser-Mitra conjecture*, *Nucl. Phys. B* **731** (2005) 109–124, [hep-th/0507275].